THREE DIMENSIONAL VERSUS TWO DIMENSIONAL LIQUEFACTION ANALYSES OF A HYDRAULIC FILL EARTH DAM

F.G. Ma[1], J. LaVassar[2], and Z.-L. Wang[3]

[1] *Geotechnical Engineer, Washington State Department of Ecology, Dam Safety Office, Spokane, WA, USA*
[2] *Geotechnical Engineer, Washington State Department of Ecology, Dam Safety Office, Olympia, WA, USA*
[3] *Senior Engineer, AMEC Geomatrix, Oakland, CA, USA*
Email: fema461@ecy.wa.gov, jlsd461@ecy.wa.gov, zlwang@gomatrix.com

ABSTRACT :

This project is a 200-foot-long, 63-foot-high earthfill dam that stores water on a seasonal basis. Deformations of the dam induced by strong ground motion and localized liquefaction were analyzed using 2D and 3D numerical models. The 2D and 3D analyses were conducted using the programs FLAC2D and FLAC^{3D} with the User Defined Model option, respectively. Since the dam spans a relative narrow valley, a 3D analysis was considered more representative than the 2D plane strain formulation. In both the 2D and 3D analyses, soil behaviors were simulated using a bounding surface plasticity model (Wang, 1990). This constitutive model simulates the shear induced contractive and dilative behaviors of sandy soils in an integrated way. The model was rewritten from the original Fortran in C++ and then compiled as a user defined model to achieve acceptable run times. In this case the deformation prediction of the 3D model was considerably less than of the 2D analysis, consistent with expectations.

KEYWORDS: earth dam, liquefaction, earthquake, plasticity model, FLAC, and FLAC^{3D}

1. PROJECT DESCRIPTION

1.1. Project History and Dam section

The 63-foot-high earth dam was built in 1910 by hydraulic fill means. Specifically, a series of earthen containment berms were placed at the upstream and downstream dam faces. Slightly gravelly, silty sand slurry was pumped into the intervening zone from spigots along either face. The dam faces are both inclined at 2.5 horizontal on 1 vertical. The crest width is 24 ft. The spillway holds the normal pool level 10 ft below the dam crest.

1.2. Constitutive Model and Implementation in FLAC

The bounding surface plasticity model (Wang 1990, or briefly, Wang model) was developed for simulating behaviors of sandy soils under complex loading conditions. Details of the model were presented in earlier papers in the reference list. Implementation of the model in FLAC involved coding the model in C++ and then compiling it as a dynamic linked library (DLL). That DLL, a user defined constitutive model (CPPUDM) can then be called in the appropriate version of FLAC (Itasca 2007) and FLAC3D (Itasca 2006). To do that the user's version of FLAC must have the User Defined Model option (an additional purchase) to run. As a CPPUDM for FLAC and FLAC^{3D}, the model has been used both as a research tool (Ma et al., 2008) and to analyze actual structures (Wang et al., 2006 and Ma et al., 2006).

2. IDEALIZED NUMERICAL MODEL OF THE DAM, MATERIAL PROPERTIES AND MODEL PARAMETERS

2.1. Idealized Dam and Foundation Grid

Figures 1 and 2 depict the 2D and 3D grids used in modeling the response of the dam. The 3D grid consists of 59392 zones. Individual zones are 10 ft by 10 ft in the x and y directions and vary from 5 to 10 ft in the z direction. The 3D dam-foundation model block has a footprint 620 ft by 560 ft and a maximum height of

160 ft. The 3D grid density not only provides a reasonable run time for a dynamic analysis, but responds to ground motions with frequencies up-to 5 HZ propagating through the soil media properly.

The 2D grid (Figure 1) is a slice of the 3D block at the maximum dam section, a section in the Y direction at x = 280 ft in Figure 2.
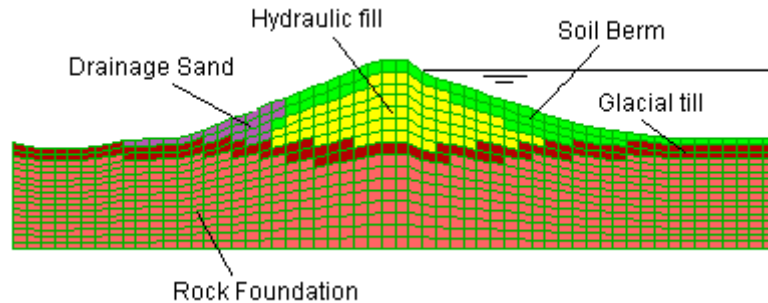
Figure 1 2D Model Grid
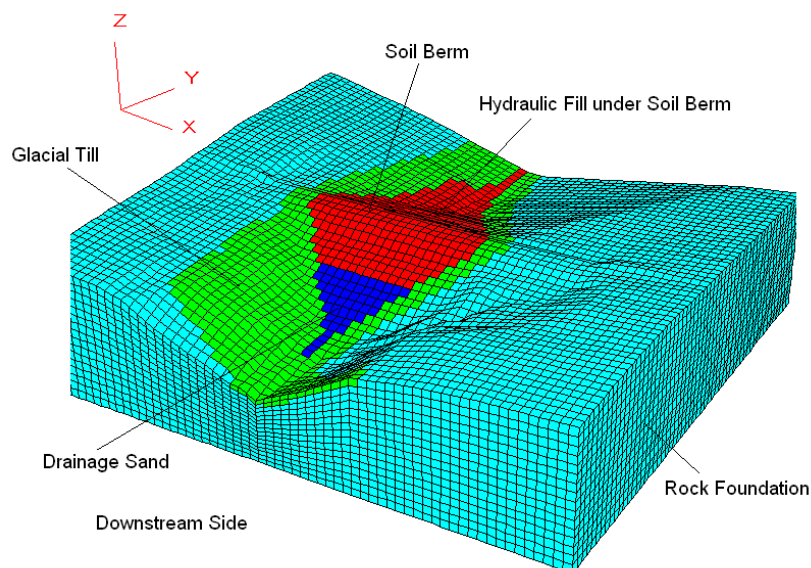
Figure 2 3D model grid

2.2. Material Properties and Model Parameters

A comprehensive yet practical constitutive model for sand (Wang 1990; Wang et al., 1990) was developed within the general framework of bounding surface plasticity. Figure 3 shows the failure surface, maximum pre-stress surface, and phase transformation line. These definitions are plotted in terms of effective mean stress, p, and the second deviatoric stress invariant, J in 3(a) and at p = const plane in 3(b). For the complete Wang model, there are total of 15 model parameters in which eight parameters are considered as 'basic' while using the model for engineering applications. Tables 1 and 2 list material properties and model parameters for this analysis, respectively.

The properties in Table 1 are self explanatory. The parameters in Table 2 are discussed below. Parameter ϕ is the effective friction angle. Parameter G_o is the modulus coefficient that defines the small strain (maximum) elastic shear modulus. Parameter h_r simulates the reduction of the shear modulus with increasing strain amplitude. Parameters k_r and d were calibrated using a trial-and-error procedure based on a typical blow count $(N_1)_{60}$ of the sand, in which k_r controls the change in effective stress during virgin loading and d controls pore pressure changes in unloading or

cyclic loading conditions. Using the selected k_r and d values, a computed soil response to cyclic loading is presented in Figure 4. Parameters λ represent soil compressibility during the isotropic virgin loading and Poisson ratio ν relates the bulk modulus to the shear modulus through the elastic equation. In Table 2, the subscript c or e refers to the value of a parameter simulating the loading condition of triaxial compression or extension, respectively. It is worth noting that Wang model parameters excluding ϕ in Table 2 are all dimensionless.
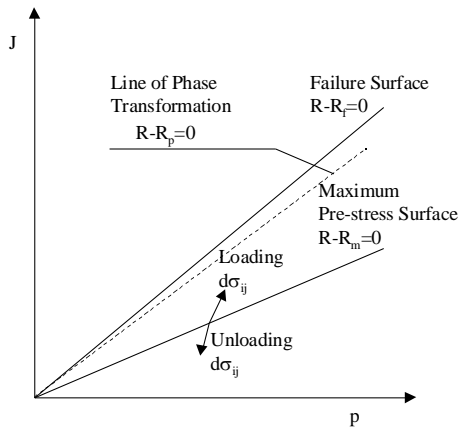
Figure 3(a) Surfaces and stress variables in J-p plane
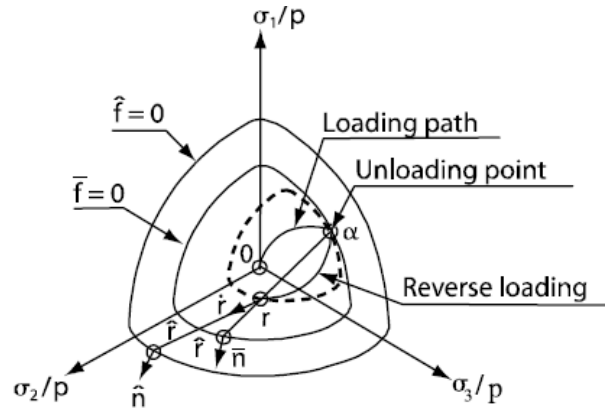
Figure 3(b) Surfaces and stress variables in p = constant plane

Other than the ones listed in Table 2, the following model parameters are set in the code with default values: $c=M_c/M_e=1$, $a=1$, $b_c= b_e =1$, $\alpha=0$, $z_n=1$, and $z_d=1$. If specific values of these parameters are necessary to simulate more complex behavior of soils (for instance, triaxial compression rather than extension), the input values of these 'secondary' parameters can overwrite the default values in the constitutive model. Also, for the three type of parameters b (b_c and b_e), h_r (h_{rc} and h_{re}), and k_r (k_{rc} and k_{re}), each type can be assigned with two values, together with $c=M_c/M_e<1$, in order to simulate soil behavior in triaxial compression versus extension.
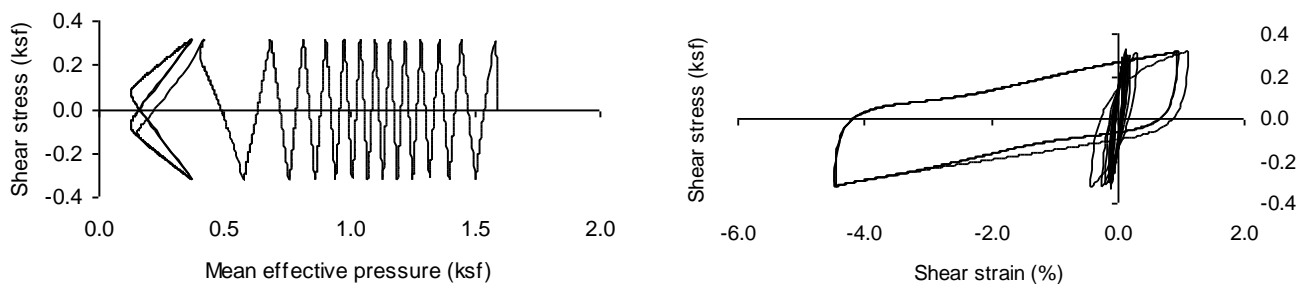
Figure 4 Computed cyclic effective stress path (left) and shear stress and shear strain relationship (right) for stress ratio = 0.2 of hydraulic fill with p_0=1.59 ksf and $(N_1)_{60} = 11$.

Table 1 Properties of the foundation and embankment soils

Properties	Rock	Glacial till	Hydraulic fill	Drainage sand	Soil Berms
Unit weight (pcf)	150	145	115	120	125
Cohesion (psf)	500	100	0.0	0.0	0.0
Friction angle (°)	45	40	37	40	40
Shear Modulus (ksf)	6600	6000	800	4900	4900
Bulk Modulus (ksf)	8800	8000	2000	7000	7000
Porosity		0.14	0.45	0.40	0.35

Table 2 Model parameters for the soils

Soil	G_0	$h_{rc}=h_{re}$	ϕ	$k_{rc}=k_{re}$	d	R_p/R_f	ν	λ
Hydraulic fill	171	0.09	37	0.5	1.5 and 2.0	0.75	0.32	0.012
Drain sand	324	0.284	40	100	100	0.75	0.30	0.012
Soil Berm	306	0.388	40	100	100	0.75	0.30	0.012

3. MODELING STEPS & SELECTION OF INPUT MOTIONS AND DYNAMIC DAMPING

Following sections present the procedures used for 2D and 3D analyses.

3.1. Static Stress Determination

Static stress and seepage analyses are required to approximate the stress state in the dam at the onset of seismic loading to obtain a reasonable distribution of initial shear moduli within the dam section. This involves setting up and running the model to achieve static balance. Then, a seepage analysis is performed to develop the phreatic surface within the dam. Finally, the mechanical effects of seepage are "turned on" to simulate their associated impact on effective stresses within the embankment. Those effective stresses are then used to calculate initial shear moduli. For the initial static analysis, a Mohr-Coulomb Model was used. For the subsequent dynamic analyses, the dam soil behavior was simulated with the Wang model.

3.2. Representative Earthquake Records

The USGS Seismic Hazard web site (http://earthquake.usgs.gov/hazmaps/) was used to determine the scenario earthquakes that contribute to the seismic risk at the site. The principal Web pages were the Interactive Deaggregation site, and the associated geographic and probabilistic deaggregation figures appropriate to Leader Lake (Long. 119.6 W, Lat. 48.3 N). For 0.5-second period spectral accelerations (approximate fundamental period of the dam-foundation system) at a return period of 2475 years, the primary contributors to the seismic risk are near-field earthquakes of moment magnitudes (M_w) 6.4 to 6.6. For the limited purposes of this study two corrected acceleration time histories were chosen from UC Berkeley's PEER Strong Motion Database. The first one is the 1980 Mammoth Lakes event in California (Mammoth Lake 5/25/80 Long Valley Dam UPR L) with peak ground acceleration of 0.27 g. The second one is the 1994 Northridge event in California (Northridge 1/17/94, 12:31, LA – Wonderland, 185, USC Station 90017) with PGA of 0.17 g. The acceleration time histories are shown in Figure 5(a) and 5(b), respectively.

(a) 1980 Ca Mammoth Earthquake   (b) 1994 Ca Northridge Earthquake
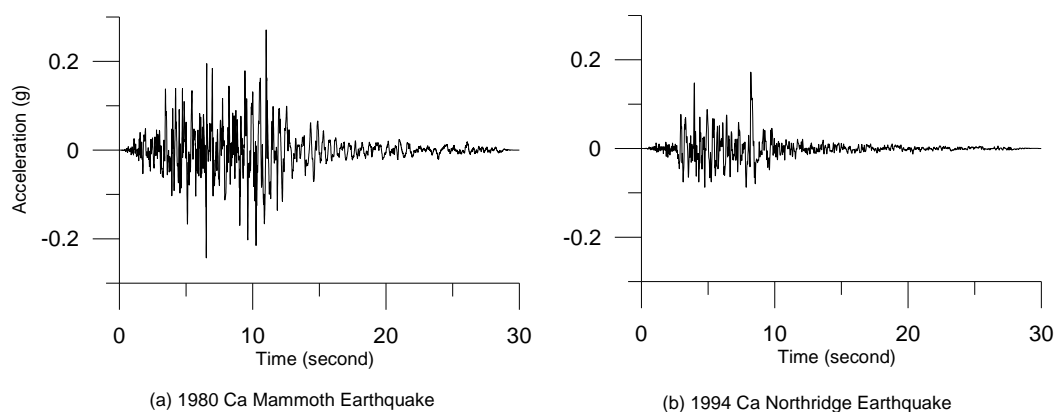
Figure 5 Input acceleration time histories

3.3. Selection of Viscous Damping of the Embankment Material

In practice, a few percent Raleigh damping has been used widely in non-linear dynamic finite element and finite

difference analyses of geotechnical problems.   In the Wang constitutive model hysteretic damping is accounted for by the non-linear model. Accordingly, Rayleigh damping was limited to 1% in the 2D & 3D analyses.

4. FLAC AND FLAC^{3D} PREDICTIONS

At the end of the 30-second earthquake time history, predicted vertical displacements of the dam crest in the 2D simulation exceeded the available freeboard (10 feet) of the dam at normal pool level. In reality, this would have resulted in overtopping of the dam and likely failure.   However, under the same earthquake loadings and material properties, the vertical deformation at the dam crest, predicted by the 3D simulation was less than 3 ft. The following presents details of the predictions from FLAC and FLAC^{3D} using the Wang model.

Figures 6 and 7 present the vertical displacement contours of the embankment using FLAC and FLAC^{3D} respectively. The seismic loading was the 1980 Mammoth Lake California earthquake with pga of 0.27g.
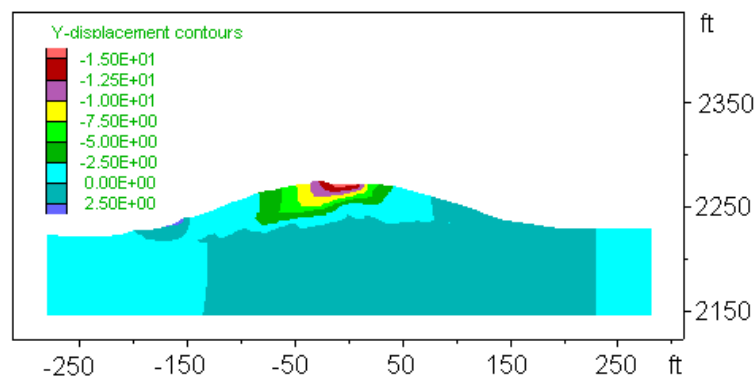
Figure 6 Predicted vertical displacement contours of FLAC2D at time = 30 seconds
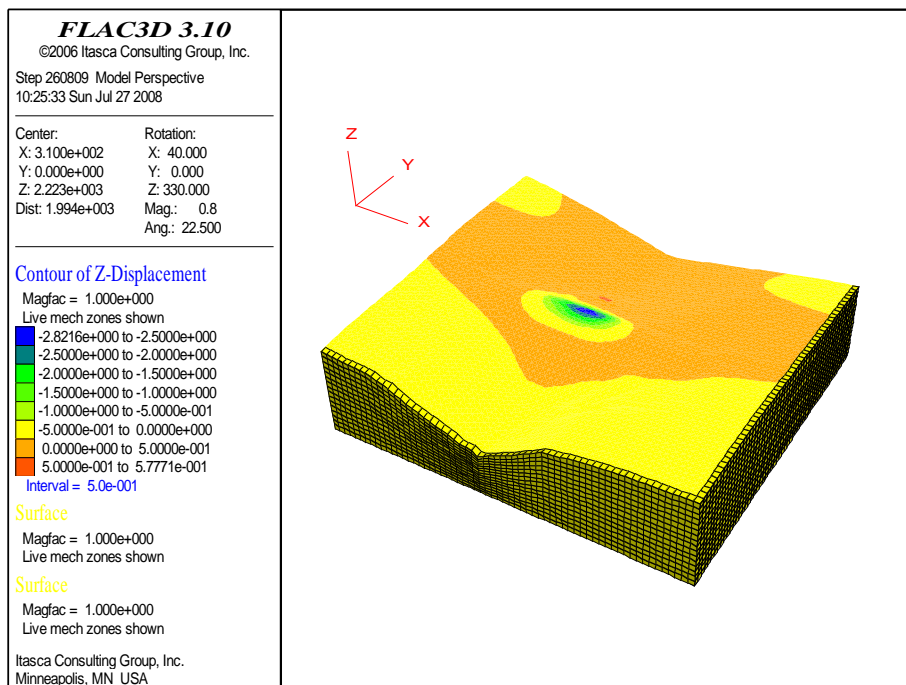
Figure 7 Predicted vertical displacement contours of FLAC^{3D} at time = 30 seconds

A comparison of Figures 6 and 7 shows that predicted vertical displacements of the dam crest using the plane strain formulation are much larger that than those of a 3D approximation. More importantly, FLAC^{3D} predicts vertical

displacements of the crest of less than 30% of the available freeboard at normal pool level. Thus, if deemed indicative of the actual dam's behavior, it likely would be judged adequate. Figure 8 presents the vertical and horizontal displacement contours on a section down the long axis of the crest centerline. The 3D analysis unlike a 2D model incorporates the constraining effects of the abutments. Fig. 9 presents time histories of the vertical displacements at a point near the center of the dam crest by FLAC and FLAC^{3D}. The maximum vertical displacement of the dam crest was more than 2 times larger (2.8 vs. 1.2 ft) with the Mammoth recording than for the Northridge quake in FLAC^{3D} analyses. However, the predicted vertical displacement was less than 30% larger with the Mammoth recording than for the Northridge quake in the 2D FLAC simulation. This is despite the fact that the PGA of the Mammoth event is about 1.6 times larger than that of Northridge while both earthquakes have similar strong motion durations (~8 seconds). Side constraint matters!
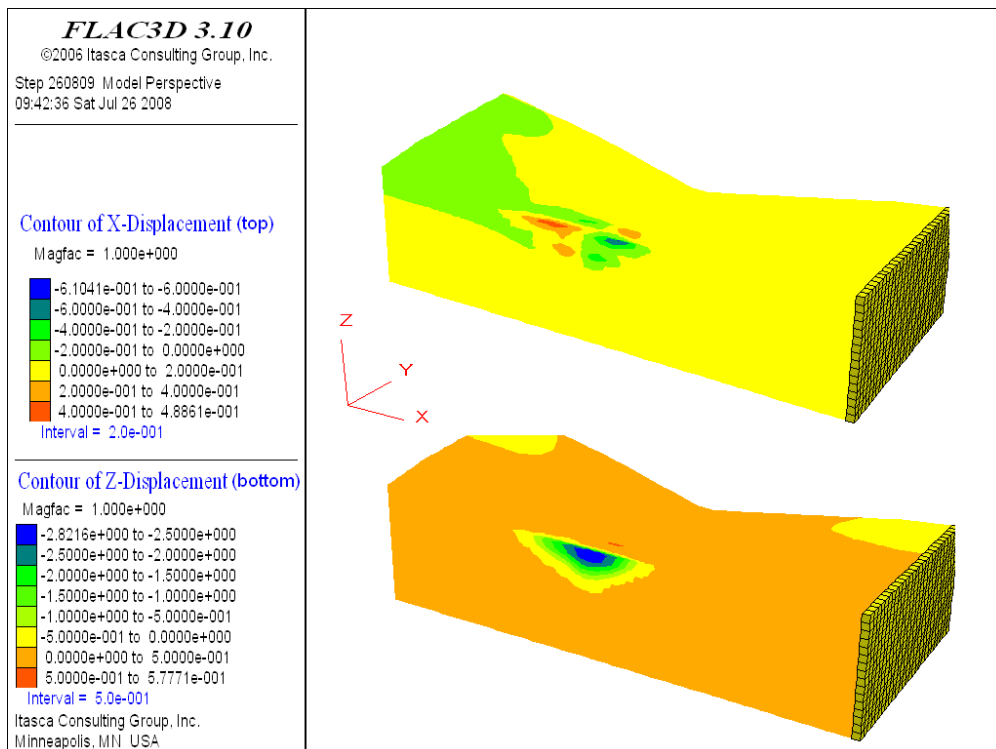
Figure 8 Vertical (Bottom) and horizontal (top) displacement contour along the dam crest.
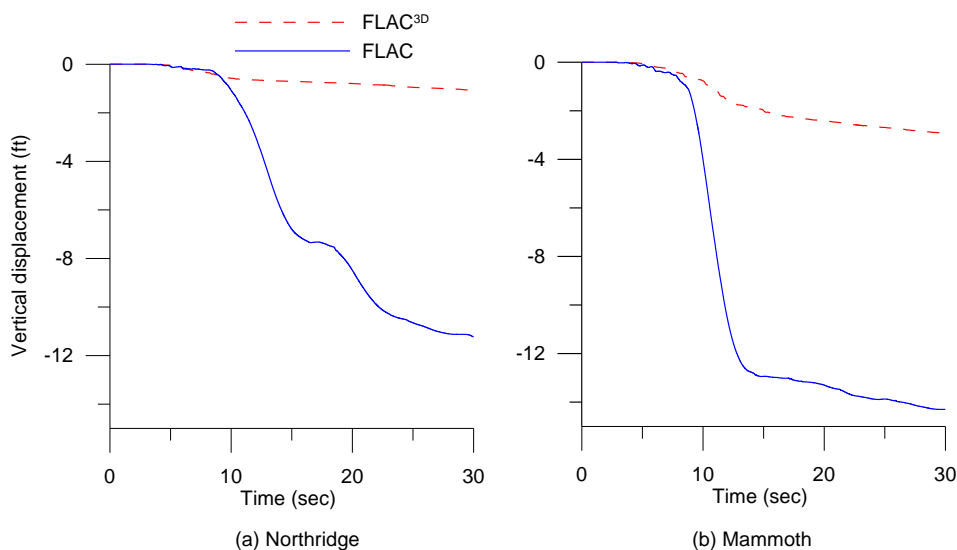
Figure 9 Vertical displacement time histories near the center of dam crest predicted using FLAC and FLAC^{3D}.

Fig. 10 presents shaking induced reduction of the mean effective confining pressure near the dam centerline (elev. 2240 ft or 40 ft below the dam crest) due to the buildup of pore water pressure from the Northridge and Mammoth earthquakes. Comparing Figures 9(a) & (b) with Figures 10(a) & (b) shows the mean effective confining pressures dropped fastest in the 3D simulations. Yet, the vertical displacements of the dam crest predicted by FLAC^{3D} did not suddenly increase due to localized liquefaction in the lower reaches of the dam section. This phenomenon demonstrates the constraining effects of the surrounding non-liquefied soil and abutments that are absent in a 2D simulation. Figure 11 presents the shear strain increment (SSI) contours from the 2D FLAC simulation. Figure 12 presents SSI contours on the equivalent sections (x=280 ft) in the 3D simulation subject to the Mammoth recording. The 2D model predicts an overall downstream orientation in sliding while the opposite is seen in the 3D modeling. The latter behavior seems more in keeping with expectations. Seismic induced stress changes in the largely saturated upstream zone would be a greater fraction of the initial stress than those acting in the downstream zone where the saturated zone is appreciable less. Those fractionally greater dynamic stresses could be expected to yield greater shear strains cycles.
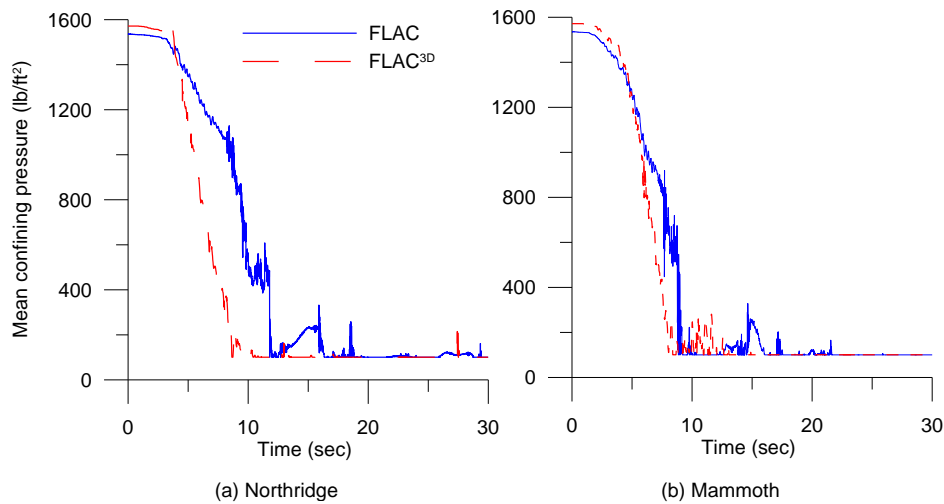
(a) Northridge   (b) Mammoth
Figure 10 Mean confining pressure reduction
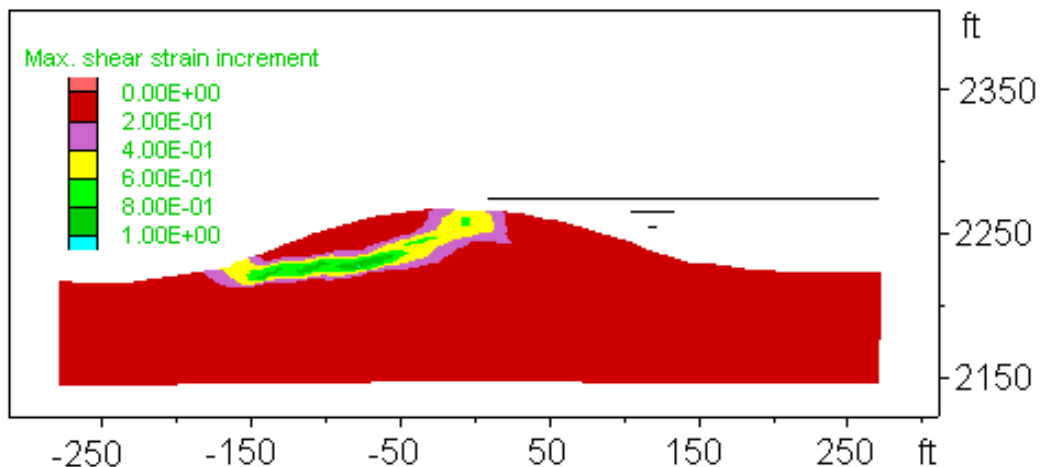
Figure 11 SSI contour at the end of the Mammoth seismic loading by FLAC

However, as presented by Fig. 13, the potential sliding surfaces during the FLAC simulations evolved from potential sliding surfaces towards both the up and downstream directions when the embankment experienced relatively smaller deformation, to the final dominating one towards the downstream direction when the embankment experienced major deformation, as demonstrated by Figs. from 13(a) to 13(b) to 12.
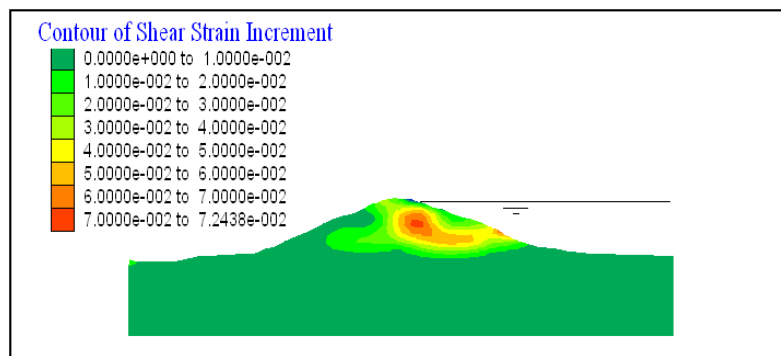
Figure 12 SSI contour at the end of the Mammoth seismic loading by FLAC^{3D} at x=280 ft
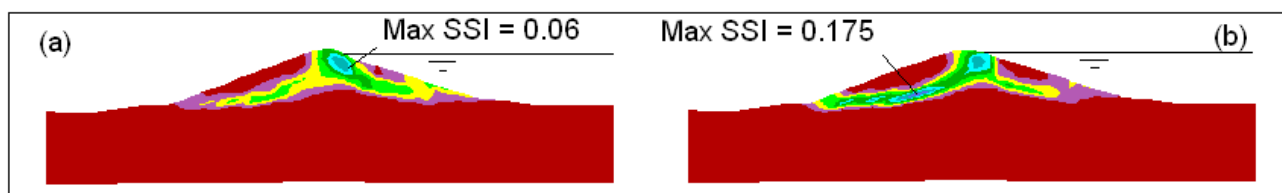
Figure 13 SSI contour at (a) 9 second with corresponding dam crest ydis=2 ft; (b) 10 second with corresponding dam crest ydis=5 ft of Mammoth earthquake by FLAC.

5. CONCLUSIONS AND LIMITATIONS

Using the 2D FLAC and FLAC^{3D}, incorporated with a bounding surface plasticity model, the dynamic analyses predicted liquefaction for an earthfill dam built across a narrow valley. FLAC predicted up-to 15 feet displacement at the dam crest. Because there are only 10 ft freeboard at normal pool of this reservoir, major retrofit would be warranted for the dam to improve the dam performance under seismic loading. However, since FLAC^{3D} only predicted less than 3-ft displacement, no retrofit effort seems necessary. Due to the drastic difference obtained from the 2D and 3D analyses, more analyses should be done to investigate effect of more earthquake records and a finer mesh before a confident conclusion can be made.

REFERENCES

CH2M Hill. 1987. Geotechnical Data Report for Leader Lake Dam. CH2M Hill.
Itasca Consulting Group, Inc. 2006. FLAC^{3D} – Fast Lagrangian Analysis of Continua in 3 Dimensions, Ver. 3.1 User's Manual. Minneapolis: Itasca.
Itasca Consulting Group, Inc. 2007. FLAC – Fast Lagrangian Analysis of Continua, Version 6 User's Manual. Minneapolis: Itasca.
Ma, F.G. and Wang, Z.L. 2008. Implementation and three dimensional example applications of a bounding surface hypo-plasticity model for sand as a C^{++} UDM for FLAC^{3D}. 1st FLAC/DEM Symposium on Numerical Modeling. 25-27 August 2008, Minneapolis, MN, USA.
Ma, F.G., Wang, Z.-L. & LaVassar, J. 2006. Liquefaction analyses of a hydraulic fill earthfill dam. In P. Varona & R. Hart (eds), FLAC and Numerical Modeling in Geomechanics – 2006, Proceedings of the Fourth International FLAC Symposium, Madrid, Spain, 29-31 May 2006, Paper #08-03. Minneapolis: Itasca.
Wang, Z.L. 1990. Bounding Surface Hypo-plasticity Model for Granular Soils and Its Application. Ph.D. Dissertation at University of California at Davis.
Wang, Z.L., Makdisi, F.I. & Egan, J. 2006. Practical Applications of a Non-linear Approach to Analysis of Earthquake-Induced Liquefaction and Deformation of Earth Structures. Journal of Soil Dynamics & Earthquake Engineering, **26(2-4)**: 231-252.